Pharmaceutical Research, Vol. 25, No. 9, September 2008 (© 2008)
DOI: 10.1007/s11095-008-9533-3

Research Paper

Plumbagin-induced Apoptosis in Human Prostate Cancer Cells is Associated with Modulation of Cellular Redox Status and Generation of Reactive Oxygen Species

Anna A. Powolny[1] and Shivendra V. Singh[1,2,3]

Received October 29, 2007; accepted January 4, 2008; published online January 23, 2008

Purpose. To investigate the mechanism of human prostate cancer cell growth inhibition by plumbagin, a constituent of the widely used medicinal herb *Plumbago zeylanica* L.
Materials and Methods. Cell viability was determined by trypan blue dye exclusion assay. Apoptosis induction was assessed by analysis of cytoplasmic histone-associated DNA fragmentation. Cell cycle distribution and generation of reactive oxygen species (ROS) were determined by flow cytometry. The effect of plumbagin treatment on cellular redox status was determined by analysis of intracellular glutathione (GSH) levels and expression of genes involved in ROS metabolism.
Results. Plumbagin treatment decreased viability of human prostate cancer cells (PC-3, LNCaP, and C4-2) irrespective of their androgen responsiveness or p53 status. Plumbagin-mediated decrease in cell viability correlated with apoptosis induction, which was accompanied by ROS generation and depletion of intracellular GSH levels. Pretreatment of cells with the antioxidant *N*-acetylcysteine inhibited plumbagin-mediated ROS generation and apoptosis. Plumbagin treatment also resulted in altered expression of genes responsible for ROS metabolism, including superoxide dismutase 2 (Mn-SOD).
Conclusion. The present study points towards an important role of ROS in plumbagin-induced apoptosis in human prostate cancer cells.

KEY WORDS: apoptosis; chemoprevention; plumbagin; prostate cancer; ROS.

INTRODUCTION

Prostate cancer is the most commonly diagnosed visceral malignancy and a leading cause of cancer related deaths among men in the United States (1). American Cancer Society predicts that nearly 219,000 new cases of prostate cancer will be diagnosed and about 27,050 men will die from this disease in the year 2007 alone. Prostate carcinogenesis is characterized by gradual transformation of normal prostate epithelium to prostatic intraepithelial neoplasia, localized tumor to advanced and metastatic disease (2). Prostate cancer is usually diagnosed in the sixth or seventh decade of life, which provides a large window of opportunity for intervention to prevent or slow disease progression. Consequently identification of novel agents that can be used to delay onset and/or progression of human prostate cancer is highly desirable.

Plumbagin (5-hydroxy-2-methyl-1,4-naphthoquinone) occurs naturally in the medicinal herb *Plumbago zeylanica* L., which has been safely used for centuries in Indian Ayurvedic and oriental medicine for treatment of various ailments, including microbial infections and allergic reactions (3–6). For example, organic solvent extract, but not the aqueous extract, of *Plumbago zeylanica* L. exhibited anti-*Helicobacter pylori* activity in agar diffusion and dilution tests (5). Plumbagin has attracted a great deal of research interest due to its diverse pharmacological effects (7–15). The known pharmacological effects of plumbagin or *Plumbago zeylanica* extract include leishmanicidal (7), anti-bacterial (8), hypolipidaemic and anti-atherosclerotic (9), and anticancer effects (11–15). For instance, dietary feeding of 200 ppm plumbagin decreased the incidence and multiplicity of azoxymethane-induced intestinal carcinogenesis in rats (12). In addition, plumbagin has been shown to be a potent radiosensitizer (16–18).

Plumbagin was recently shown to suppress activation of nuclear factor-κB (NF-κB) and NF-κB-regulated gene expression through modulation of p65 and IκBα kinase in KBM-5 human chronic myeloid leukemia, U937 myeloid lymphoma, H1299 lung adenocarcinoma, A293 human kidney carcinoma, and SCC-4 human squamous cell carcinoma cells (19). Plumbagin-mediated suppression of NF-κB activation was accompanied by potentiation of apoptosis induced by

[1] Department of Pharmacology and Urology, University of Pittsburgh Cancer Institute, University of Pittsburgh School of Medicine, Pittsburgh, Pennsylvania, USA.
[2] 2.32A Hillman Cancer Center Research Pavilion, 5117 Centre Avenue, Pittsburgh, Pennsylvania 15213, USA.
[3] To whom correspondence should be addressed. (e-mail: singhs@upmc.edu)

ABBREVIATIONS: DCF, 2′,7′-dichlorofluorescein; DMSO, dimethyl sulfoxide; FBS, fetal bovine serum; GSH, glutathione; H_2DCFDA, 6-carboxy-2′,7′-dichlorodihydrofluorescein diacetate; Mn-SOD, manganese superoxide dismutase; NAC, *N*-acetylcysteine; NF-κB, nuclear factor-κB; PBS, phosphate buffered saline; ROS, reactive oxygen species.

cytokines and chemotherapeutic agents (19). The NF-κB is a transcription factor involved in regulation of various genes including inflammatory cytokines, chemokines, cell adhesion molecules, and growth factors (20). This transcription factor regulates gene expression of a number of anti-apoptotic proteins including c-IAP2, ch-IAP1, Bfl-1/A1, and survivin (21–24). The NF-κB is constitutively activated in a variety of hematological and solid tumor cells including prostate cancer cells (25–28).

Because plumbagin treatment suppresses NF-κB activation (19), we hypothesized that this phytochemical might reduce viability of human prostate cancer cells. In the present study, we tested this hypothesis using PC-3 (an androgen-independent cell line lacking functional p53), LNCaP (an androgen-responsive cell line expressing wild-type p53), and C4-2 (an androgen-independent variant of LNCaP cells) human prostate cancer cell lines as a model. We demonstrate that plumbagin treatment decreases viability of cultured human prostate cancer cells regardless of their androgen responsiveness or p53 status. Contrary to previous reports (14, 15), plumbagin exposure fails to activate G2/M phase checkpoint in the prostate cancer cell lines tested in the present study. Instead, plumbagin-mediated suppression of prostate cancer cell viability correlated with apoptotic cell death characterized by cytoplasmic histone-associated DNA fragmentation. We also provide experimental evidence to indicate that the plumbagin-induced apoptosis in our model is associated with alteration in cellular redox status and generation of reactive oxygen species (ROS).

MATERIALS AND METHODS

Reagents. Plumbagin was purchased from Sigma (St. Louis, MO). 6-carboxy-2′,7′-dichlorodihydrofluorescein diacetate (H_2DCFDA) was from Invitrogen (Carlsbad, CA), RNaseA, propidium iodide and *N*-acetylcysteine (NAC) were from Sigma. The antibodies against manganese-superoxide dismutase (Mn-SOD) and catalase were purchased from Calbiochem (Ann Arbor, MI), while anti-actin antibody was from Sigma. RPMI-1640 was from Cellgro (Herndon, VA). Other cell culture reagents, including the non-heat-inactivated fetal bovine serum (FBS) were from Gibco Invitrogen.

Cell culture and cell viability assay. The LNCaP (American Type Culture Collection) and C4-2 cells (UroCor) were maintained in RPMI 1640 medium supplemented with 1 mM sodium pyruvate, 10 mM HEPES, 0.24% glucose, 10% (*v*/*v*) FBS, and antibiotics. The PC-3 cells (American Type Culture Collection) were maintained in F-12K nutrient mixture (Kaighn's modification) supplemented with 7% (*v*/*v*) FBS and antibiotics. Stock solution of plumbagin was prepared in dimethyl sulfoxide (DMSO) and diluted with medium. An equal volume of DMSO (final concentration <0.1%) was added to the controls. Effect of plumbagin treatment on cell viability was determined by trypan blue dye exclusion assay as described by us previously (29).

Determination of cell cycle distribution and apoptosis induction. The effect of plumbagin treatment on cell cycle distribution was determined by flow cytometric analysis of nuclear DNA content after staining the cells with propidium iodide. Briefly, LNCaP, C4-2 and PC-3 cells were seeded at a density of 3×10^5 and allowed to attach by overnight incubation. The medium was replaced with fresh complete medium containing desired concentrations of plumbagin or DMSO (control). After desired time of plumbagin exposure at 37°C, floating and adherent cells were collected, washed with phosphate-buffered saline (PBS), and fixed with 70% ice-cold ethanol. The fixed cells were treated with 80 μg/ml RNaseA and 50 μg/ml propidium iodide for 30 min at room temperature. The stained cells were analyzed using a Coulter Epics XL Flow Cytometer (Miami, FL). Cells in different phases of the cell cycle (G0/G1, S, G2/M and sub-diploid apoptotic fraction) were computed for control (DMSO-treated) and plumbagin-treated PC-3, LNCaP and C4-2 cultures. Apoptosis in control (DMSO-treated) and plumbagin-treated PC-3, LNCaP, and C4-2 cultures was quantified by measurement of release of histone-associated DNA fragments into the cytosol using a kit from Roche Applied Science (Indianapolis, IN) according to the manufacturer's instructions. In some experiments, cells were pretreated for 2 h with 4 mM NAC, washed with PBS, and then exposed to plumbagin prior to analysis of histone-associated DNA fragmentation.

Measurement of intracellular ROS generation. Intracellular ROS generation was measured by flow cytometry following staining with H_2DCFDA as described by us previously with some modifications (30). Briefly, cells were plated at a density of 3×10^5, allowed to attach by overnight incubation, and exposed to DMSO or specified concentrations of plumbagin for 1–8 h. Cells were stained with 20 μM H_2DCFDA for 30 min at 37°C, collected by trypsinization, and the fluorescence was measured by flow cytometry. In some experiments, cells were pretreated for 2 h with 4 mM NAC, washed with PBS, and then exposed to plumbagin prior to ROS measurement.

Total RNA extraction and gene expression analysis. Total RNA was extracted from LNCaP cells treated with DMSO (control) or 7.5 μM plumbagin for 8 h using the RNeasy Kit (Qiagen, Valencia, CA). Reverse transcription was performed using 2–3 μg of RNA and SuperScript III First-Strand Synthesis System for RT-PCR (Invitrogen, Carlsbad, CA). The Human Oxidative Stress and Antioxidant Defense RT^2 Profiler™ PCR Array (SuperArray Biosciences, Frederic, MD) was used to evaluate the effect of plumbagin on expression of genes involved in ROS metabolism. Experimental cocktail mix, prepared immediately before the real time analyses, included cDNA sample and SYBR green probe. A 25 μl of the cocktail mix was added into each well of the 96-well plate, including the control wells. A two-step cycling protocol was used on a ABI 700 cycler (Foster City, CA; 10 min at 95°C followed by 40 cycles of 15 s at 95°C and 1 min at 60°C). The data were analyzed using the software provided by the manufacturer. The threshold cycle (C_t) values for each well were calculated and genes with C_t values above 35 were considered undetected. Baseline and threshold values were manually set at the same levels for different analyses to allow for comparison of multiple plates. A set of three house keeping genes was used to normalize the

results (HPRT, GAPDH, and β-actin). For each sample, the C_t values for each gene were adjusted for the average C_t values of the housekeeping genes (ΔC_t). The $\Delta\Delta C_t$ value for each gene was calculated as a difference between the ΔC_t for plumbagin treated and control samples.

Measurement of glutathione levels. The effect of plumbagin treatment on intracellular glutathione (GSH) levels was determined using Glutathione Assay Kit (Cayman Chemical, Ann Arbor, MI) according to the manufacturer's protocol. Briefly, LNCaP cells (1×10^6) were plated in 100-mm culture dishes, allowed to attach overnight, and exposed to desired concentrations of plumbagin for specific time periods. Cells were harvested, counted, washed with PBS, and suspended in 1 ml ice-cold solution containing 50 mM 2-(*N*-morpholino) ethanesulphonic acid and 1 mM EDTA. The cells were disrupted by homogenization and centrifuged at 10,000×*g* for 15 min at 4°C. Supernatant fraction was then removed and deproteinated using metaphosphoric acid followed by centrifugation at 2,000×*g* for 2 min. A 500 µl aliquot of the supernatant fraction was mixed with 25 µl of 4 M triethanolamine. Standard and test samples were pipetted onto 96 well plate. Manufacturer supplied assay cocktail was prepared fresh and added to each well. Samples were then incubated at room temperature for 5–30 min with shaking and absorbance was measured every 5 min at 405 nm using a microplate reader (Labsystems Multiscan Plus, Franklin, MA). Concentration of GSH in test samples was determined based on the standard curve and adjusted for the dilution and the number of cells in each sample.

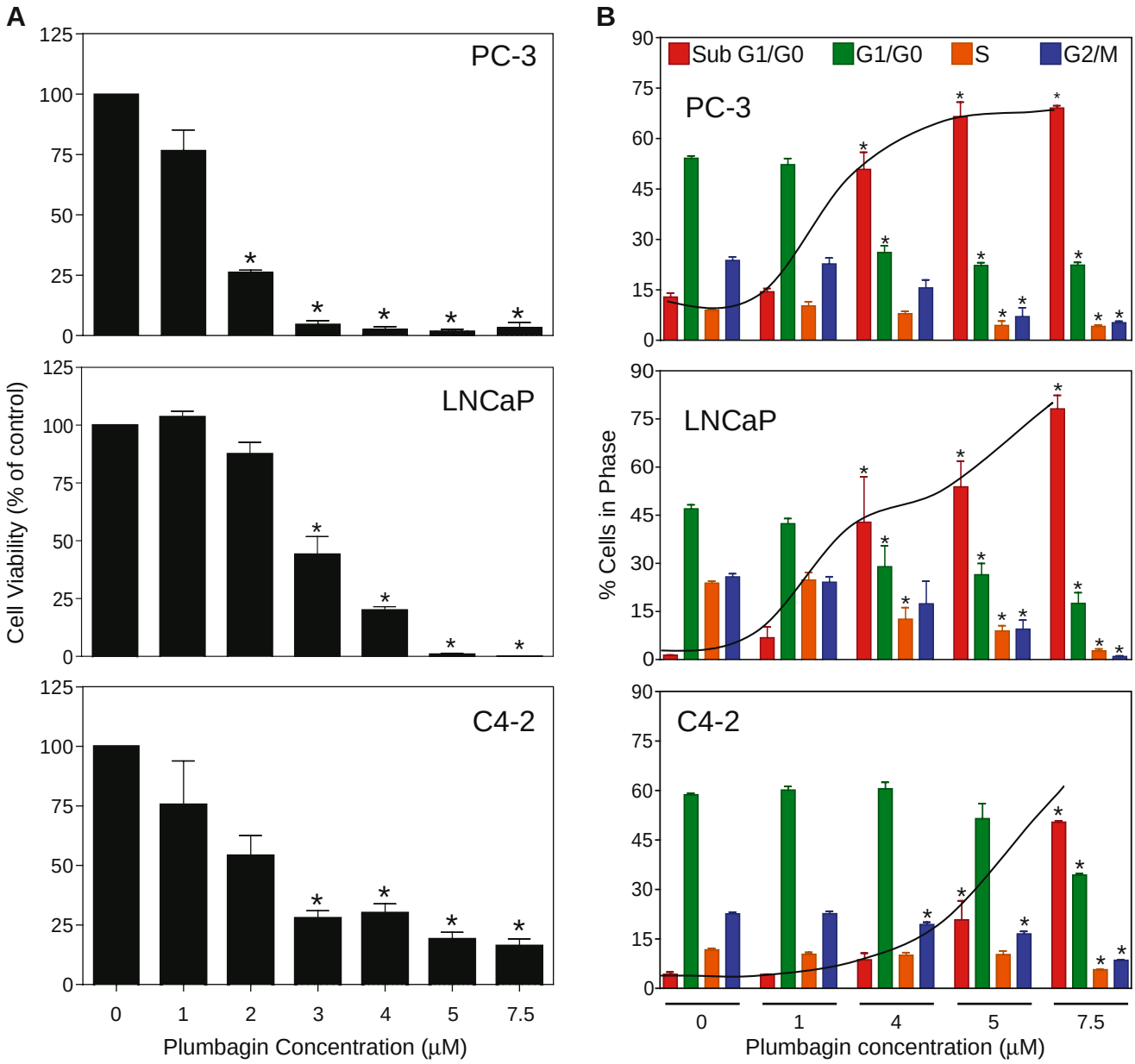

Fig. 1. Effect of plumbagin treatment (24 h exposure) on **A** viability and **B** cell cycle distribution of PC-3, LNCaP and C4-2 cells. Results are mean±SE (n=3). *Significantly different (P<0.05) compared with DMSO-treated control by one-way ANOVA followed by Dunnett's test. Similar results were observed in at least two independent experiments.

Measurement of SOD and catalase activities. The effects of plumbagin treatment on SOD and catalase activities were determined using Superoxide Dismutase Assay and Catalase Assay kits from Cayman Chemical. Cells exposed to DMSO (control) or desired concentrations of plumbagin were collected, counted and homogenized in a solution containing 20 mM HEPES, 1 mM EGTA, 210 mM mannitol and 70 mM sucrose for SOD activity and 50 mM potassium phosphate, 1 mM EDTA (pH 7.0) for catalase activity. Cellular extracts were centrifuged at 15,000×*g* for 5 min and the resultant supernatant fractions were used for measurement of SOD and catalase activities according to the manufacturer's protocol.

Immunoblotting. The LNCaP cells (1×10^6) were plated in 100-mm culture dishes, allowed to attach overnight, and exposed to DMSO (control) or desired concentrations of plumbagin for specified time periods. The cell lysate preparation and immunoblotting were performed as described by us previously (29,30). Immunoreactive bands were visualized using the enhanced chemiluminescence method. The change in protein level was determined by densitometric analyses of the immunoreactive bands and corrected for the actin loading control.

RESULTS

Plumbagin treatment decreased viability of human prostate cancer cells. We conducted trypan blue dye exclusion assay to probe into the questions of whether (a) plumbagin affected viability of cultured human prostate cancer cells, and (b) effect of plumbagin treatment on prostate cancer cell viability was influenced by androgen responsiveness or p53 status. We addressed these questions using a panel of well-characterized human prostate cancer cell lines, including PC-3, LNCaP, and C4-2. The PC-3 cell line is androgen-independent and lacks functional p53 (31). In contrast, the LNCaP cell line is androgen responsive and expresses wild type p53 (31). The C4-2 cell line is an androgen-independent variant of LNCaP cells and was generated through co-culture of parental cells with human bone fibroblasts *in vivo* in castrated male athymic mice (32,33). These cells display elevated prostate-specific antigen expression and increased anchorage-independent growth in soft agar (32,33). As shown in Fig. 1A, plumbagin treatment decreased viability of each cell line in a dose dependent manner. The concentrations of the plumbagin used for cell viability assays were selected from previous publications in other cell lines and a pharmacokinetic study in rats (13–15,34). Based on these results, we concluded that the plumbagin-mediated decrease in prostate cancer cell viability was not affected by androgen responsiveness or p53 status. The IC_{50} for plumbagin in PC-3, LNCaP and C4-2 cells varied between 2 and 3 μM and was within the range reported in MDA-MB-231 and MCF-7 human breast cancer and ME-180 cervical cancer cell lines (13,14).

Plumbagin treatment caused apoptosis in human prostate cancer cells. Previous studies have shown that growth suppressive effect of plumbagin against human breast cancer cell lines MDA-MB-231 and MCF-7 correlates with G2/M phase cell cycle arrest (6 h treatment with 4 and 8 μM plumbagin) due to checkpoint kinase 2 and cell division cycle 25C-dependent inactivation of cyclin-dependent kinase 1 (14). The G2/M phase cell cycle arrest upon treatment of A549 human lung cancer cell line with 10 and 20 μM plumbagin for 6 h has also been reported (15). We proceeded to test whether plumbagin-mediated decrease in prostate cancer cell viability was associated with G2/M phase cell cycle arrest. As can be

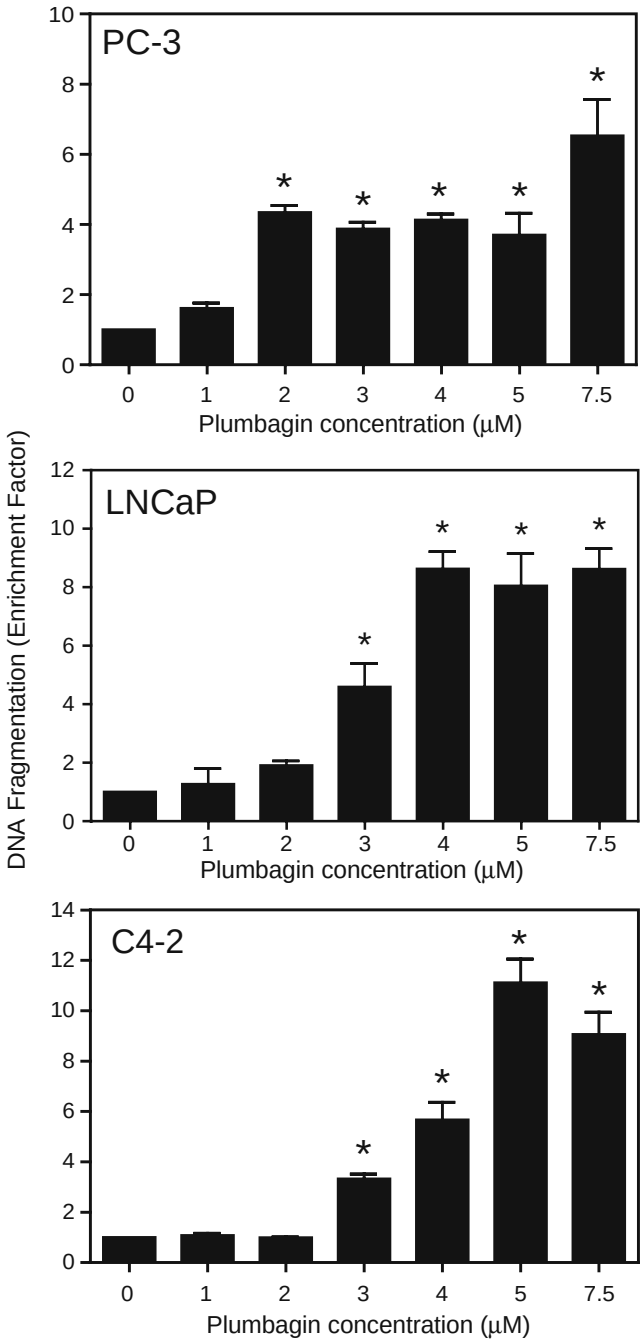

Fig. 2. Release of histone-associated DNA fragments into the cytosol in response to treatment with increasing concentrations of plumbagin in PC-3, LNCaP and C4-2 cells. Results are mean±SE ($n=3$). *Significantly different ($P<0.05$) compared with DMSO-treated control by one-way ANOVA followed by Dunnett's test. Similar results were observed in at least two independent experiments.

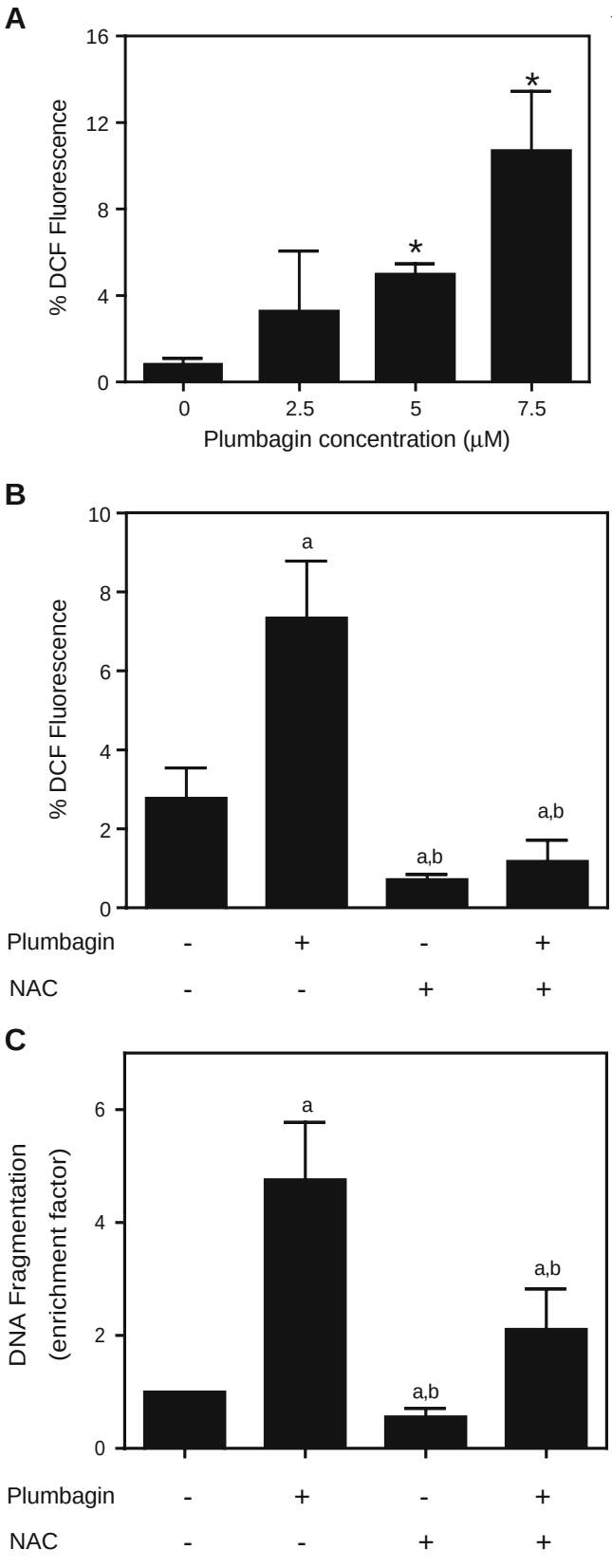

Fig. 3. **A** Plumbagin treatment causes ROS generation in LNCaP cells in a dose-dependent manner. Columns show mean fold change relative to DMSO-treated control and bars represent SE. *Significantly different ($P<0.05$) compared with DMSO-treated control by one-way ANOVA followed by Dunnett's test. Pretreatment of LNCaP cells with NAC inhibits plumbagin-mediated **B** ROS generation and **C** apoptotic DNA fragmentation. Columns represent mean and bars represent SE. Significantly different ($P<0.05$) compared with *a* DMSO-treated control, and *b* plumbagin alone treatment group by one-way ANOVA followed by Bonferroni's multiple comparison test. Experiments were repeated at least twice with comparable results.

seen in Fig. 1B, plumbagin treatment (24 h treatment) failed to cause G2/M phase cell cycle arrest in any of the three cell lines examined in the present study. Since the plumbagin-mediated G2/M phase cell cycle arrest in breast and lung cancer cells was observed 6 h post-treatment (14,15) we conducted a detailed time-course kinetic study using PC-3, LNCaP and C4-2 cells. The percentage of G2/M fraction did not differ significantly between DMSO-treated control and plumbagin-treated PC-3, LNCaP or C4-2 cells at 4, 8, or 16 h time points (results not shown). Instead, the plumbagin-treated PC-3, LNCaP and C4-2 cultures revealed statistically significant increase in sub-diploid fraction, an indicator of apoptotic cell death, compared with corresponding DMSO-treated controls (Fig. 1B). The plumbagin-mediated enrichment of sub-diploid apoptotic fraction in each cell line was accompanied by a decrease in G0/G1, S, and/or G2/M populations (Fig. 1B).

Previous studies showed that plumbagin treatment caused apoptotic cell death in ME-180 human cervical cancer and A549 human lung cancer cell lines (13,15). On the other hand, plumbagin-mediated suppression of MDA-MB-231 and MCF-7 human breast cancer cell growth was mainly attributable to type II autophagic death but not apoptosis (14). We therefore proceeded to test whether plumbagin-mediated decrease in prostate cancer cell viability was due to apoptosis. We addressed this question by determining the effect of plumbagin treatment on release of histone-associated DNA fragments into the cytosol, which is a well-accepted technique for quantitation of apoptosis. A 24 h exposure of PC-3, LNCaP, and C4-2 cells to plumbagin resulted in a marked and statistically significant increase in release of histone-associated DNA fragments into the cytosol compared with DMSO-treated control (Fig. 2). The plumbagin-mediated release of histone-associated DNA fragments into the cytosol was clearly evident at 3–7.5 μM concentrations (Fig. 2). These results indicated that, unlike human breast cancer cells (14), plumbagin-mediated suppression of prostate cancer cell growth was due to apoptosis induction. Since cellular responses to plumbagin (cell growth inhibition and apoptosis induction) were comparable in the three cell lines, we focused on LNCaP cells for further mechanistic studies.

Plumbagin-induced apoptosis correlated with ROS generation. Recent studies from our laboratory have revealed that ROS serve as critical signaling intermediates in apoptosis induction by various natural products including garlic constituent diallyl trisulfide, cruciferous vegetable derived isothiocyanates and Indian Ayurvedic medicine constituent guggulsterone (30,35–38). The plumbagin-induced apoptosis in human cervical cancer cell line ME-180 also correlated with ROS generation (13). Therefore, we raised the question of whether plumbagin-induced apoptosis in our model was linked to ROS generation. To address this question, initially

we determined ROS generation following treatment of LNCaP cells with plumbagin. Intracellular ROS generation in plumbagin-treated cells was determined by flow cytometry after staining the cells with H_2DCFDA, which is cleaved by nonspecific esterases and oxidized in presence of peroxides (e.g., hydrogen peroxide) to yield fluorescent 2′,7′-dichlorofluorescein (DCF). As shown in Fig. 3A, exposure of LNCaP cells to plumbagin resulted in a concentration-dependent increase in DCF fluorescence compared with DMSO-treated control. In time course experiments using 4 μM plumbagin, increase in DCF fluorescence over DMSO-treated control was evident at 4 and 8 h time points (results not shown). To probe into the question of whether ROS generation contributed to apoptosis in our model, we determined the effect of NAC pretreatment (4 mM for 2 h) on plumbagin-induced ROS generation and apoptosis. As can be seen in Fig. 3B, the plumbagin-mediated increase in DCF fluorescence in LNCaP cells was completely abolished by pretreatment with NAC. Moreover, NAC pretreatment conferred partial yet statistically significant protection against plumbagin-mediated histone-associated DNA fragmentation (Fig. 3C). These results clearly indicated that the plumbagin-induced apoptosis in LNCaP cells was linked to ROS generation.

Plumbagin treatment altered expression of genes involved in ROS metabolism. Since the plumbagin-mediated ROS generation and apoptosis was significantly attenuated in the presence of NAC (Fig. 3B–C), we proceeded to determine the mechanism of ROS generation in our model by measuring the effect of plumbagin treatment on expression of genes involved in ROS metabolism. Because plumbagin-mediated ROS generation was maximal after 8 h of treatment, we selected this time point for gene expression analysis. The effect of plumbagin treatment on expression of genes involved in ROS metabolism was determined using RT^{2}Profiler PCR array, which can detect expression of over eighty

Table I. Effect of Plumbagin on Expression of Genes Involved in ROS Metabolism

Gene name	UniGene	Ref sequence	Fold change relative to control
Up-regulated genes			
Angiopoietin-like 7	Hs.146559	NM_021146	2.88
ATX1 antioxidant protein 1 homolog (yeast)	Hs.125213	NM_004045	6.41
Chemokine (C-C motif) ligand 5	Hs.514821	NM_002985	5.47
Cytochrome b-245, alpha polypeptide	Hs.513803	NM_000101	3.05
Dual oxidase 1	Hs.272813	NM_175940	3.64
Dual oxidase 2	Hs.71377	NM_014080	3.63
Dual specificity phosphatase 1	Hs.171695	NM_004417	6.12
Eosinophil peroxidase	Hs.279259	NM_000502	3.07
Glutathione peroxidase 2 (gastrointestinal)	Hs.2704	NM_002083	3.35
Glutathione peroxidase 3 (plasma)	Hs.386793	NM_002084	2.81
Glutathione peroxidase 5	Hs.248129	NM_001509	8.82
Glutathione peroxidase 6 (olfactory)	Hs.448570	NM_182701	9.71
Glutathione peroxidase 7	Hs.43728	NM_015696	8.85
Keratin 1 (epidermolytic hyperkeratosis)	Hs.80828	NM_006121	10.90
Lactoperoxidase	Hs.234742	NM_006151	9.71
Mannose-binding lectin (protein C) 2, soluble	Hs.499674	NM_000242	8.93
Myeloperoxidase	Hs.458272	NM_000250	6.58
Metallothionein 3	Hs.73133	NM_005954	6.96
Neutrophil cytosolic factor 1	Hs.458275	NM_000265	7.53
Neutrophil cytosolic factor 2	Hs.518604	NM_000433	4.95
Nitric oxide synthase 2A (inducible)	Hs.462525	NM_000625	5.39
Phosphoinositide-binding protein PIP3-E	Hs.146100	NM_015553	2.59
Phosphatidylinositol-3,4,5-trisphosphate-dependent RAC exchanger 1	Hs.153310	NM_020820	5.31
Proteoglycan 3	Hs.251386	NM_006093	7.13
Prostaglandin-endoperoxide synthase 2	Hs.196384	NM_000963	6.98
Peroxidasin homolog-like (*Drosophila*)	Hs.444882	NM_144651	8.39
Superoxide dismutase 3, extracellular	Hs.2420	NM_003102	4.94
Sulfiredoxin 1 homolog (*S. cerevisiae*)	Hs.516830	NM_080725	3.37
Thyroid peroxidase	Hs.467554	NM_000547	9.37
Titin	Hs.134602	NM_003319	2.74
Thioredoxin domain containing 2	Hs.98712	NM_032243	6.02
Down-regulated genes			
Arachidonate 12-lipoxygenase	Hs.567231	NM_000697	−2.30
24-dehydrocholesterol reductase	Hs.498727	NM_014762	−2.28
Epoxide hydrolase 2, cytoplasmic	Hs.212088	NM_001979	−2.01
Superoxide dismutase 2, mitochondrial	Hs.487046	NM_000636	−50.06
General transcription factor II,	Hs.520459	NM_001518	−1.96
Catalase	Hs.502302	NM_001752	−1.97

Cells were treated with DMSO or 7.5 μM plumbagin for 8 h at 37°C. Cells were collected, total RNA was extracted, and reverse transcription was performed as described in the methods section. Results are mean fold change (n=2 for control group and n=3 for plumbagin treated samples). Statistical analyses were performed using the software provided by the manufacturer.

genes. Our analyses revealed that plumbagin treatment up-regulated expression of over 30 genes and down-regulated 6 genes in LNCaP cells. As can be seen in Table I, the up-regulated genes included a variety of peroxidases (e.g., glutathione peroxidases, myeloperoxidase, and thyroid peroxidase). Down-regulated genes included catalase and Mn-SOD (the mitochondrial form of SOD). These results indicated that plumbagin affected metabolism of ROS by changing mRNA levels of a variety of genes including peroxidases, catalase, and SOD.

Plumbagin treatment decreased intracellular GSH levels. Reduced GSH is the major non-protein thiol in cells and is essential for maintaining cellular redox status. Since plumbagin-induced apoptosis in human prostate cancer cells correlated with ROS generation, we argued that plumbagin treatment might disturb cellular redox status. To address this issue, we determined the effect of plumbagin treatment on intracellular GSH levels. Plumbagin treatment resulted in depletion of intracellular GSH levels in LNCaP cells in a time- (Fig. 4A; 7.5 μM plumbagin) and dose-dependent (Fig. 4B; 8 h treatment) manner. These experiments supported the notion that plumbagin treatment affected cellular redox status.

Effect of plumbagin treatment on SOD and catalase activities. Next, we designed experiments to verify the results of gene expression analyses. We focused on Mn-SOD since plumbagin treatment had maximal effect on expression of this gene. As can be seen in Fig. 5A, treatment of LNCaP cells with 7.5 μM plumbagin resulted in suppression of total SOD activity, which was most pronounced and statistically significant at the 8 h time point. The plumbagin-mediated suppression of SOD activity was also observed at 5 μM concentration (Fig. 5B). Consistent with the results of gene expression analysis (Table I) and enzyme activity determination (Fig. 5B), treatment of LNCaP cells with 5 and 7.5 μM plumbagin for 8 h resulted in a marked decrease in the levels of Mn-SOD protein (Fig. 5C). We also determined the effect of plumbagin treatment on catalase activity as a negative control since its gene expression was only marginally decreased upon treatment of LNCaP cells with plumbagin (Table I). As can be seen in Fig. 5D, plumbagin treatment did not have an appreciable effect on catalase activity. Consistent with these results, the protein level of catalase was not altered in plumbagin-treated LNCaP cells (results not shown).

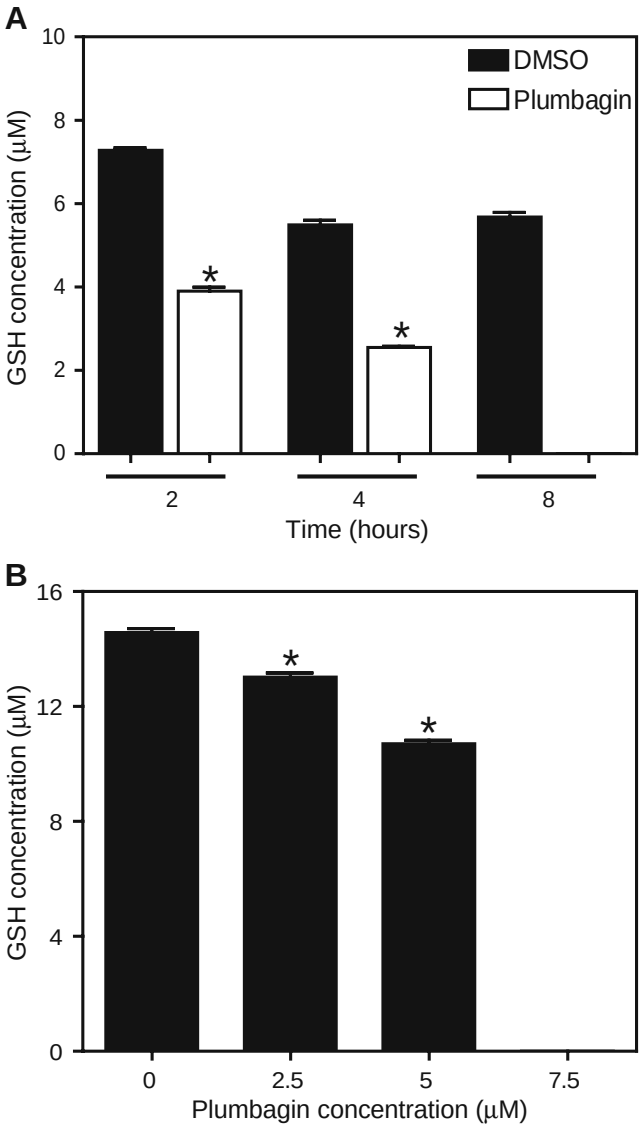

Fig. 4. Plumbagin treatment depletes intracellular GSH levels in a **A** time- (7.5 μM plumbagin) and **B** dose-dependent manner (8 h treatment). *Columns* represent mean and *bars* represent the SE value ($n=3$). *Significantly different ($P<0.05$) compared with DMSO-treated control by paired *t*-test (**A**) or one-way ANOVA followed by Dunnett's test (**B**). Similar results were observed in at least two independent experiments.

DISCUSSION

The present study demonstrates that plumbagin is effective against proliferation of cultured human prostate cancer cells irrespective of their androgen responsiveness. To the best of our knowledge, the present study is the first published report to document growth suppressive effect of plumbagin, which has been safely used for centuries in traditional Ayurvedic and Chinese medicine to treat variety of ailments, against prostate cancer cells. It is interesting to note that plumbagin decreases viability of human prostate cancer cells containing wild-type p53 (LNCaP) as well as cells lacking p53 (PC-3), which is in contrast to previous studies suggesting involvement of p53 in cellular responses to plumbagin (15). In addition, contrary to previous reports in MDA-MB-231 and MCF-7 human breast cancer cells and A549 human lung cancer cell line (14,15) plumbagin treatment failed to activate G2/M phase cell cycle arrest in human prostate cancer cell lines examined in the present study (Fig. 1B). We conclude that p53-dependence and activation of G2/M phase cell cycle arrest are probably cell-line specific responses unique to MDA-MB-231, MCF-7 and A549 cells.

We found that the plumbagin-mediated decrease in prostate cancer cell viability correlates with ROS-dependent apoptosis induction. This conclusion is supported by our observations that plumbagin causes ROS generation in a dose-dependent manner and the ROS generation as well as apoptotic DNA fragmentation resulting from treatment with

plumbagin is significantly attenuated in the presence of NAC. Moreover, plumbagin treatment results in imbalance of cellular redox status as revealed by depletion of primary non-protein thiol GSH and changes in expression of genes involved in ROS metabolism (e.g., Mn-SOD). Further studies are needed to probe into the molecular mechanism for plumbagin-mediated changes in expression of different antioxidant genes. Similarly, studies are also needed to determine the mechanism(s) by which ROS generation contributes to the apoptosis induction by plumbagin. One possibility to explain the positive correlation between ROS generation and apoptosis induction by plumbagin relates to activation of multi-domain pro-apoptotic protein Bax. Previous studies have shown that ROS generation by certain stimuli leads to conformational change and mitochondrial translocation (activation) of Bax (39). It is also possible that plumbagin-mediated ROS generation activates c-Jun N-terminal kinase, which is pro-apoptotic and involved in activation of Bax (40, 41). It is interesting to note that activation of c-Jun N-terminal kinase upon treatment of A549 human lung cancer cells with plumbagin has been demonstrated previously (15). However, probing into these speculations requires further investigation.

The plumbagin-mediated growth inhibition, ROS generation, and apoptosis induction are evident at 3–7.5 μM concentrations (Figs. 1, 2 and 3). A key question relevant to further clinical development of plumbagin is whether the concentrations of this agent required for suppression of prostate cancer growth are achievable in humans. Even though plasma levels of plumbagin in humans have not yet been determined, oral bioavailability of plumbagin was measured in a conscious freely moving rat (34). The maximal plasma concentration (C_{max}) of plumbagin in rat following treatment with 3 mg/kg i.v. and 100 mg/kg p.o. was shown to be about 1.0 and 1.85 μM with corresponding $t_{1/2}$ of about 108 and 1028 min, respectively (34). The oral

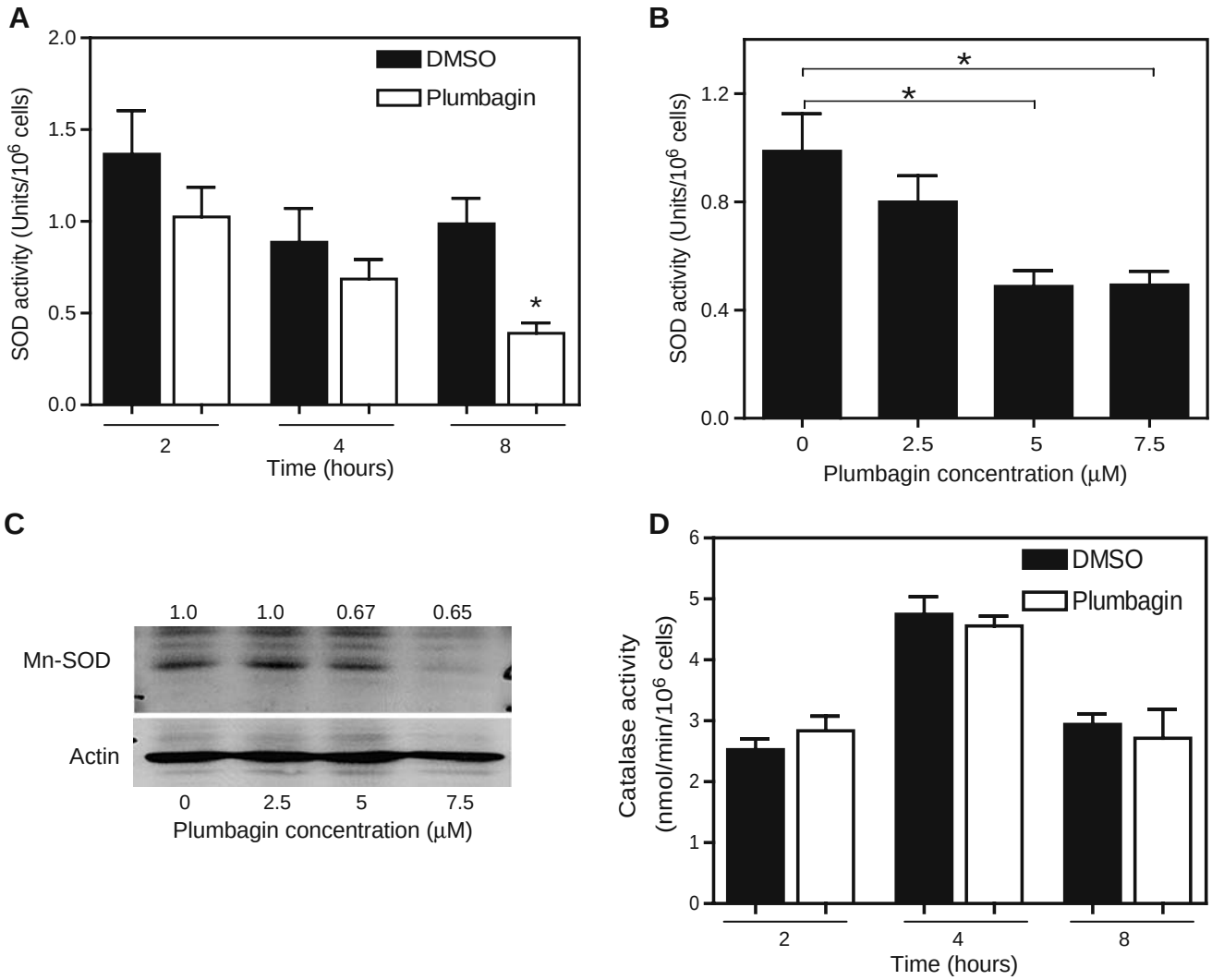

Fig. 5. The Mn-SOD activity in LNCaP cells treated with **A** DMSO (control) or 7.5 μM plumbagin for the indicated time periods or **B** the indicated concentrations of plumbagin for 8 h. **C** Immunoblotting for effect of plumbagin treatment (8 h) on Mn-SOD protein levels. Membrane was stripped and re-probed with anti-actin antibody to ensure equal protein level. Change in Mn-SOD protein level relative to control is shown on top of each band. **D** Catalase activity in LNCaP cells treated with DMSO (control) or 7.5 μM plumbagin for the indicated time periods. *Significantly different ($P<0.05$) compared with DMSO-treated control by paired *t*-test (**A**) or one-way ANOVA followed by Dunnett's test (**B**). Similar results were observed in at least two independent experiments.

bioavailability [$(AUC_{po}/Dose_{po})/(AUC_{iv}/Dose_{iv})$] of plumbagin was about 38.7±5% (34). Thus, it is possible that the concentrations of plumbagin needed for prostate cancer cell growth inhibition may be achievable in humans by repeated dosing schedule.

CONCLUSIONS

In conclusion, the results of the present study indicate that plumbagin reduces viability of human prostate cancer cells by induction of apoptosis but without affecting cell cycle progression. Additionally, we demonstrated that plumbagin-induced apoptosis is mediated by ROS generation and accompanied by an imbalance in cellular redox status.

ACKNOWLEDGMENTS

This investigation was supported by the National Cancer Institute (NCI) grant CA115498.

REFERENCES

1. A. Jemal, R. Siegel, E. Ward, T. Murray, J. Xu, and M. J. Thun. Cancer statistics. *CA Cancer J. Clin* **57**:43–66 (2007).
2. W. G. Nelson, A. M. De Marzo, and W. B. Isaacs. Prostate cancer. *N. Engl. J. Med* **349**:366–381 (2003).
3. N. Y. Chiu, and K. H. Chang. The illustrated medicinal plants of Taiwan. SMC, Taipei, 1986, p. 172.
4. Y. C. Wang, and T. L. Huang. Screening of anti-*Helicobacter pylori* herbs deriving from Taiwanese folk medicinal plants. *FEMS Immunol. Med. Microbiol* **43**:295–300 (2005).
5. Y. C. Wang, and T. L. Huang. Anti-*Helicobacter pylori* activity of *Plumbago zeylanica* L. *FEMS Immunol. Med. Microbiol* **43**:407–412 (2005).
6. Y. Dai, L. F. Hou, Y. P. Chan, L. Cheng, and P. P. But. Inhibition of immediate allergic reactions by ethanol extract from *Plumbago zeylanica* stems. *Biol. Pharm. Bull* **27**:429–432 (2004).
7. M. J. Chan-Bacab, and L. M. Pena-Rodriguez. Plant natural products with leishmanicidal activity. *Nat. Prod. Rep* **18**:674–688 (2001).
8. M. Krishnaswamy, and K. K. Purushothaman. Plumbagin: A study of its anticancer, antibacterial & antifungal properties. *Indian J. Exp. Biol* **18**:876–877 (1980).
9. I. Sharma, D. Gusain, and V. P. Dixit. Hypolipidaemic and antiatherosclerotic effects of plumbagin in rabbits. *Indian J. Physiol. Pharmacol* **35**:10–14 (1991).
10. R. Parimala, and P. Sachdanandam. Effect of Plumbagin on some glucose metabolizing enzymes studied in rats in experimental hepatoma. *Mol. Cell. Biochem* **125**:59–63 (1993).
11. R. A. Naresh, N. Udupa, and P. U. Devi. Niosomal plumbagin with reduced toxicity and improved anticancer activity in BALB/C mice. *J. Pharm. Pharmacol* **48**:1128–1132 (1996).
12. S. Sugie, K. Okamoto, K. M. Rahman, T. Tanaka, K. Kawai, J. Yamahara, and H. Mori. Inhibitory effects of plumbagin and juglone on azoxymethane-induced intestinal carcinogenesis in rats. *Cancer Lett* **127**:177–183 (1998).
13. P. Srinivas, G. Gopinath, A. Banerji, A. Dinakar, and G. Srinivas. Plumbagin induces reactive oxygen species, which mediate apoptosis in human cervical cancer cells. *Mol. Carcinog* **40**:201–211 (2004).
14. P. L. Kuo, Y. L. Hsu, and C. Y. Cho. Plumbagin induces G2-M arrest and autophagy by inhibiting the AKT/mammalian target of rapamycin pathway in breast cancer cells. *Molecular Cancer Therapeutics* **5**:3209–3221 (2006).
15. Y. L. Hsu, C. Y. Cho, P. L. Kuo, Y. T. Huang, and C. C. Lin. Plumbagin (5-hydroxy-2-methyl-1,4-naphthoquinone) induces apoptosis and cell cycle arrest in A549 cells through p53 accumulation via c-Jun NH2-terminal kinase-mediated phosphorylation at serine 15 *in vitro* and *in vivo*. *J. Pharmacol. Exp. Ther* **318**:484–494 (2006).
16. P. U. Devi, B. S. Rao, and F. E. Solomon. Effect of plumbagin on the radiation induced cytogenetic and cell cycle changes in mouse Ehrlich ascites carcinoma *in vivo*. *Indian J. Exp. Biol* **36**:891–895 (1998).
17. A. Ganasoundari, S. M. Zare, and P. U. Devi. Modification of bone marrow radiosensensitivity by medicinal plant extracts. *Br. J. Radiol* **70**:599–602 (1997).
18. V. S. Prasad, P. U. Devi, B. S. Rao, and R. Kamath. Radiosensitizing effect of plumbagin on mouse melanoma cells grown *in vitro*. *Indian J. Exp. Biol* **34**:857–858 (1996).
19. S. K. Sandur, H. Ichikawa, G. Sethi, K. S. Ahn, and B. B. Aggarwal. Plumbagin (5-hydroxy-2-methyl-1,4-naphthoquinone) suppresses NF-kappaB activation and NF-kappaB-regulated gene products through modulation of p65 and IkappaBalpha kinase activation, leading to potentiation of apoptosis induced by cytokine and chemotherapeutic agents. *J. Biol. Chem* **281**:17023–17033 (2006).
20. S. Miyamoto, and I. M. Verma. Rel/NF-kappa B/I kappa B story. *Adv. Cancer Res* **66**:255–292 (1995).
21. Z. L. Chu, T. A. McKinsey, L. Liu, J. J. Gentry, M. H. Malim, and D. W. Ballard. Suppression of tumor necrosis factor-induced cell death by inhibitor of apoptosis c-IAP2 is under NF-kappaB control. *Proc. Natl. Acad. Sci. U. S. A* **94**:10057–10062 (1997).
22. M. You, P. T. Ku, R. Hrdlickova, and H. R. Bose. ch-IAP1, a member of the inhibitor-of-apoptosis protein family, is a mediator of the antiapoptotic activity of the v-Rel oncoprotein. *Mol. Cell. Biol* **17**:7328–7341 (1997).
23. W. X. Zong, L. C. Edelstein, C. Chen, J. Bash, and C. Gelinas. The prosurvival Bcl-2 homolog Bfl-1/A1 is a direct transcriptional target of NF-kappaB that blocks TNFalpha-induced apoptosis. *Genes Dev* **13**:382–387 (1999).
24. L. Zhu, S. Fukuda, G. Cordis, D. K. Das, and N. Maulik. Anti-apoptotic protein survivin plays a significant role in tubular morphogenesis of human coronary arteriolar endothelial cells by hypoxic preconditioning. *FEBS Lett* **508**:369–374 (2001).
25. R. C. Bargou, F. Emmerich, D. Krappmann, K. Bommert, M. Y. Mapara, W. Arnold, H. D. Royer, E. Grinstein, A. Greiner, C. Scheidereit, and B. Dörken. Constitutive nuclear factor-kappaB-RelA activation is required for proliferation and survival of Hodgkin's disease tumor cells. *J. Clin. Invest* **100**:2961–2969 (1997).
26. R. L. Shattuck-Brandt, and A. Richmond. Enhanced degradation of I-kappaB alpha contributes to endogenous activation of NF-kappaB in Hs294T melanoma cells. *Cancer Res* **57**:3032–3039 (1997).
27. G. Dong, Z. Chen, T. Kato, and C. van Waes. The host environment promotes the constitutive activation of nuclear factor-kappaB and proinflammatory cytokine expression during metastatic tumor progression of murine squamous cell carcinoma. *Cancer Res* **59**:3495–3504 (1999).
28. S. T. Palayoor, M. Y. Youmell, S. K. Calderwood, C. N. Coleman, and B. D. Price. Constitutive activation of IkappaB kinase alpha and NF-kappaB in prostate cancer cells is inhibited by ibuprofen. *Oncogene* **18**:7389–7394 (1999).
29. D. Xiao, S. Choi, D. E. Johnson, V. G., Vogel, C. S. Johnson, D. L. Trump, Y. J. Lee, and S. V. Singh. Diallyl trisulfide-induced apoptosis in human prostate cancer cells involves c-Jun N-terminal kinase and extracellular-signal regulated kinase-mediated phosphorylation of Bcl-2. *Oncogene* **23**:5594–5606 (2004).
30. S. V. Singh, S. K. Srivastava, S. Choi, K. L. Lew, J. Antosiewicz, D. Xiao, Y. Zeng, S. C. Watkins, C. S. Johnson, D. L. Trump, Y. J. Lee, H. Xiao, and A. Herman-Antosiewicz. Sulforaphane-induced cell death in human prostate cancer cells is initiated by reactive oxygen species. *J. Biol. Chem* **280**:19911–19924 (2005).
31. M. M. Webber, D. Bello, and S. Quader. Immortalized and tumorigenic adult human prostatic epithelial cell lines: characteristics and applications. Part 3. Oncogenes, suppressor genes, and applications. *Prostate* **30**:136–142 (1997).

32. G. N. Thalmann, P. E. Anezinis, S. M. Chang, H. E. Zhau, E. E. Kim, V. L. Hopwood, S. Pathak, A. C. von Eschenbach, and L. W. Chung. Androgen-independent cancer progression and bone metastasis in the LNCaP model of human prostate cancer. *Cancer Res* **54**:2577–2581 (1994).
33. H. C. Wu, J. T. Hsieh, M. E. Gleave, N. M. Brown, S. Pathak, and L. W. Chung. Derivation of androgen-independent human LNCaP prostatic cancer cell sublines: role of bone stromal cells. *Int. J. Cancer* **57**:406–412 (1994).
34. Y. J. Hsieh, L. C. Lin, and T. H. Tsai. Measurement and pharmacokinetic study of plumbagin in a conscious freely moving rat using liquid chromatography/tandem mass spectrometry. *J. Chromatogr. B* **844**:1–5 (2006).
35. D. Xiao, K. L. Lew, Y. Zeng, H. Xiao, S. W. Marynowski, R. Dhir, and S. V. Singh. Phenethyl isothiocyanate-induced apoptosis in PC-3 human prostate cancer cells is mediated by reactive oxygen species-dependent disruption of the mitochondrial membrane potential. *Carcinogenesis* **27**:2223–2234 (2006).
36. D. Xiao, V. Vogel, and S. V. Singh. Benzyl isothiocyanate-induced apoptosis in human breast cancer cells is initiated by reactive oxygen species and regulated by Bax and Bak. *Molecular Cancer Therapeutics* **5**:2931–2945 (2006).
37. Y. A. Kim, D. Xiao, H. Xiao, A. A. Powolny, K. L. Lew, M. L. Reilly, Y. Zeng, Z. Wang, and S. V. Singh. Mitochondria-mediated apoptosis by diallyl trisulfide in human prostate cancer cells is associated with generation of reactive oxygen species and regulated by Bax/Bak. *Molecular Cancer Therapeutics* **6**:1599–1609 (2007).
38. S. V. Singh, S. Choi, Y. Zeng, E. Hahm, and D. Xiao. Guggulsterone-induced apoptosis in human prostate cancer cells is caused by reactive oxygen intermediate-dependent activation of c-Jun NH_2-terminal kinase. *Cancer Res* **67**:7439–7449 (2007).
39. L. J. Buccellato, M. Tso, O. I. Akinci, N. S. Chandel, and G. R. S. Budinger. Reactive oxygen species are required for hyperoxia-induced Bax activation and cell death in alveolar epithelial cells. *J. Biol. Chem* **279**:6753–6760 (2004).
40. R. J. Davis. The mitogen-activated protein kinase signal transduction pathway. *J. Biol. Chem* **268**:14553–14556 (1993).
41. K. Lei, and R. J. Davis. JNK phosphorylation of Bim-related members of the Bcl2 family induces Bax-dependent apoptosis. *Proc. Natl. Acad. Sci. U. S. A* **100**:2432–2437 (2003).